**Physical Sciences**

Original article

# Influence of process parameters on the size, morphology, and structure of magnetic nanoparticles obtained by chemical methods

## Influencia de los parámetros de proceso en el tamaño, morfología y estructura de nanopartículas magnéticas obtenidas mediante métodos químicos

**Nicolás Ortiz-Godoy[1,*], Dayi Gilberto Agredo-Diaz[1], Jimmy Rene Junco[1], David Arsenio Landínez-Téllez[2], Jairo Roa-Rojas[2]**

[1] Departamento de Ingeniería Mecánica y Mecatrónica, Facultad de Ingeniería, Universidad Nacional de Colombia, Bogotá, Colombia
[2] Grupo de Física de Nuevos Materiales, Departamento de Física, Universidad Nacional de Colombia, Bogotá, Colombia

## Abstract

In the last decade, magnetic nanomaterials have been widely used in the fields of chemistry, physics, engineering, and medicine due to their optical, magnetic, and conductive properties, and as contrast agents in magnetic resonance. Their influence in the treatment of cancerous tumors has been evaluated and has sparked great interest in its use in environmental repair systems such as magnetic absorbers that trap metal particles and some contaminants. Here we analyze the influence of process parameters to obtain magnetic nanoparticles under three chemical synthesis methods. Its morphological characterization was performed by scanning electron microscopy (SEM), its elemental composition by energy dispersive spectroscopy (EDS), and its structure by x-ray diffraction (XRD). Our results showed that the obtention method had a great influence as evidenced by the variability in nanoparticle sizes. It is worth highlighting that we obtained particles at a nanometric scale, especially $Fe_3O_4$ (magnetite) and $Fe_2O_3$ (maghemite) structures, with potential superparamagnetism properties that could open a wide range of future applications for the production of these materials at low cost and easy access.

**Keywords:** Magnetic nanoparticles; Magnetite; Maghemite; SEM; XRD.

## Resumen

En la última década los nanomateriales magnéticos se han utilizado ampliamente en el campo de la química, la física, la ingeniería y la medicina debido a sus propiedades ópticas, magnéticas y de conducción, y como agentes de contraste en resonancia magnética. Se ha evaluado su influencia en el tratamiento de tumores cancerosos y está despertando gran interés en sistemas de reparación ambiental como absorbentes magnéticos que atrapan partículas de metal y algunos contaminantes. En este estudio se analizó la influencia de los parámetros de proceso en la obtención de nanopartículas magnéticas bajo tres métodos de síntesis química. La caracterización morfológica se hizo por microscopía electrónica de barrido (SEM), su composición elemental se estudió mediante espectroscopia de energía dispersiva de rayos x (EDS), y su estructura, mediante difracción de rayos x (XRD). Los resultados evidenciaron una gran influencia del método de obtención, como se reflejó en la variabilidad del tamaño de las nanopartículas. Es de resaltar la obtención de partículas a escala nanométrica, con predominancia de estructuras $Fe_3O_4$ (magnetita) y $Fe_2O_3$ (maghemita), lo cual supondría propiedades de superparamagnetismo que abrirían el camino a un amplio abanico de aplicaciones futuras con su producción a bajo costo y de fácil acceso.

**Palabras clave:** Nanopartículas magnéticas; Magnetita; Maghemita; MEB; DRX.

**Citation:** Nicolás Ortiz-Godoy, Dayi Gilberto Agredo-Diaz, Jimmy Rene Junco, *et al.* Influence of process parameters on the size, morphology, and structure of magnetic nanoparticles obtained by chemical methods. Rev. Acad. Colomb. Cienc. Ex. Fis. Nat. 44(173):951-959, octubre-diciembre de 2020. doi: https://doi.org/10.18257/raccefyn.1223

**Editor:** Gabriel Téllez Acosta

***Corresponding autor:**
Nicolás Ortiz Godoy;
nortizg@unal.edu.co

**Received:** May 22, 2020
**Accepted:** July 30, 2020
**Published:** December 5, 2020

doi: https://doi.org/10.18257/raccefyn.1223

## Introduction

Recently, studies have centered on nanomaterials with magnetic behavior that have different applications in physics, chemistry, and medicine due to their optical properties, as well as in other fields (**Blanco-Gutiérrez, *et al.,*** 2013; **Kisan, *et al*.,** 2014; **Blanco-Gutiérrez, *et al.,*** 2010; **López-Ruiz, *et al.,*** 2012; **Muñoz, *et al.,*** 2013). They are also used as a contrast in vascular diagnostic imaging (**Bakenecker, *et al*.,** 2020), like temperature sensors in MRI (**Hankiewicz *et al.,*** 2019), and as an alternative treatment for patients with cancerous tumors through magnetic fluid hyperthermia (MFH) (**Benhal, *et al.,*** 2019). In environmental remediation, their ability to retain metals and contaminants, such as chromium VI in contaminated water resulting from the corrosion caused by the stainless-steel present in nuclear reactor shells, has been tested as well, which is vital given the risk it represents for the environment and human health (**Ismail, *et al.,*** 2019). Similarly, they have proven useful to detect *Salmonella* in milk quickly and efficiently (**Jin, *et al.,*** 2020) and in the processing of cooking oil waste to make biodiesel using magnetic nanoparticles as a catalyst (**Touqeer, *et al.,*** 2020).

Magnetic nanoparticles can be obtained by chemical and physical methods (**Wang & Zhang,** 2020), using a hydrothermal method based on low-temperature coprecipitation (**Chellappa & Vijayalakshmi,** 2019), or by self-combustion (**Sontu, *et al.,*** 2018).

Within the wide variety of magnetic nanoparticles, iron oxides such as magnetite $Fe_3O_4$ and maghemite $Fe_2O_3$ stand out due to their stability and accessibility. Magnetite is stable in the pH range between 8 and 14 in an environment where no oxidation is present. The composition has a ratio of 2:1 of $Fe^{3+}$ and $Fe^{2+}$ ions whereas if the process is carried out in a potentially oxidizing environment what maghemite is obtained (**Toma, *et al.,*** 2016).

In the present study, we compared three chemical methods for obtaining magnetic Fe nanoparticles, each of them with a different degree of difficulty. We specifically compared their effectiveness in obtaining a homogeneous morphology and nanometric scale and an adequate elemental composition, i.e., with no contamination of the precursor elements of the process and with a highly crystalline structure.

One of the synthesis methods discussed in our study was coprecipitation in an aqueous medium without temperature, which has a medium-level complexity and can be carried out in a standard laboratory. This method was used by **Arévalo, *et al.*** (2017) with a great variety of precursors, such as polymeric surfactants, polyvinyl alcohol, and others, and they achieved a high level of reliability in the synthesis of particles with nanometric dimensions and spinel structure, which is characteristic of magnetite. Other researchers obtained similar results when using this method with different precursors (**Houshiar, *et al.,*** 2014; **Iranmanesh, *et al.,*** 2018; **Raeisi-Shahraki, *et al.,*** 2012).

The second synthesis method we analyzed was the obtention of magnetic Fe nanoparticles by using ferrous sulfate as the main precursor for coprecipitation at a constant temperature of 90°C. A similar process using the same main precursor but a different chemical synthesis method was conducted by **Tao, *et al*.** (2020). In their study, they made the physicochemical analysis of the sustainable production of Fe2O3 nanoparticles from the reduction of ferrous sulfate with coke, thereby optimizing the sulfur recycling process resulting from the obtention of white titanium (**Ren, *et al*.,** 2017). The third method we explored was coprecipitation without temperature where the precursor is an alternative element such as iron filings obtained from nails or wires and immersed in an acidic medium, such as vinegar, for a period of 12 to 24 hours (**Toma, *et al*.,** 2016).

## Materials and methods

Nanoparticles were obtained through three synthesis methods which we describe below:

### *Synthesis method 1*

In this method, we used coprecipitation in an aqueous medium without temperature mixing the $Fe^{2+}$ and $Fe^{3+}$ precursors in an alkaline medium (**Toma, *et al.,*** 2016). First, we prepared

doi: https://doi.org/10.18257/raccefyn.1223

two solutions in distilled water in beakers: one with 1.079 M de $FeSO_4$ $7H_2O$ and another with 2.1458 M de $FeCl_3$ $6H_2O$. These two solutions were then mixed using a mechanical agitator with a polymer impeller at 1000 rpm for 5 minutes. Subsequently, we prepared a solution with 0.3 M de NaOH in distilled water and added it to the previously made mixture, we then incorporated the three solutions and stirred again at 1000 rpm until the initially orange mixture changed to black, after which we continued to stir for another 15 minutes. Once the mechanical agitation finished, magnetic nanoparticles (MNP) were separated using a neodymium magnet, subsequently decanted with acetone, and, finally, completely dried by applying temperature on a watch glass to eliminate all the humidity. **Figure 1** shows an outline of the method.

### *Synthesis method 2*

**Figure 2** shows an outline of the second synthesis method where we used a mechanical stirrer with a polymer impeller and a temperature plate to maintain a constant temperature of 80 to 90°C in the mixture throughout the stirring process. The $66x10^{-3}$ M solution of $FeSO_4$ $7H_2O$ was prepared in distilled water and mixed with two previously prepared solutions: the first one with $56.05x10^{-3}$ M de $KNO_3$ and the second one with 1.485 M de KOH, both in distilled water. Then the beaker with the mixture was placed on the preheated plate, the temperature was quickly stabilized between 80 and 90°C, and, then, the mixture was stirred at 1000 rpm. When we started the mixing of the three solutions, the color was green which later turned to black due to the reactions produced by the agitation and the temperature. After this color was reached, we continued agitating for 20 minutes and, finally, we checked the alkaline pH of the product at a range between 12 and 14. Then the NPMs were separated using a neodymium magnet and decanted with acetone for their subsequent drying (**Toma, *et al*.,** 2016).

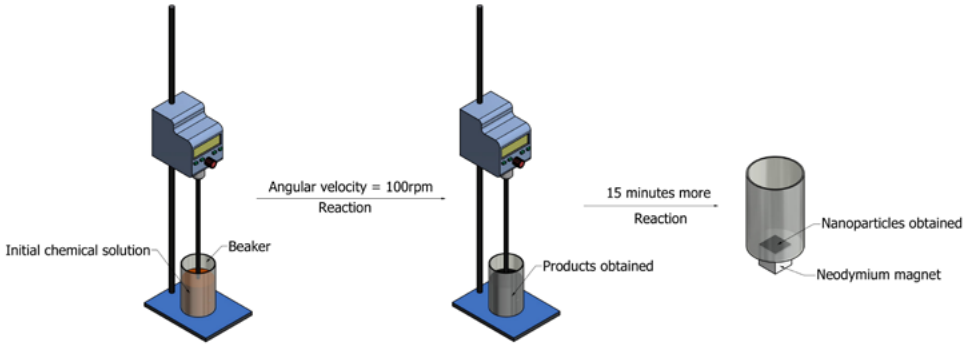


**Figure 1.** Simplified scheme of synthesis method 1

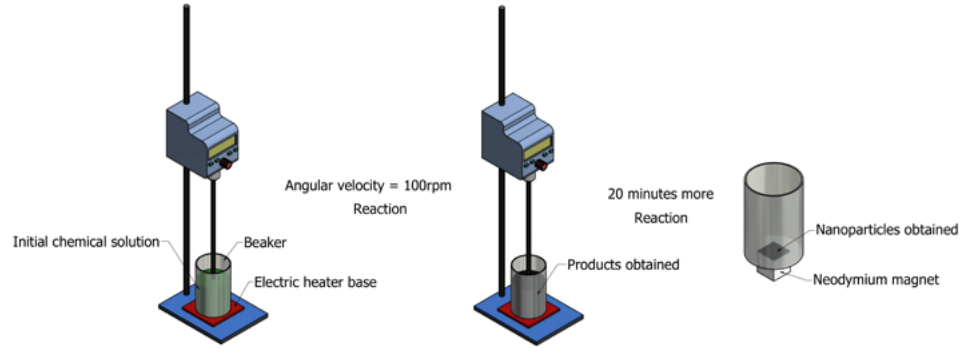


**Figure 2.** Simplified scheme of synthesis method 2

doi: https://doi.org/10.18257/raccefyn.1223

### *Synthesis method 3*

For the development of the third method, a lance was used as the main precursor, which was kept immersed in a beaker with vinegar for a period of 24 hours to obtain an iron solution. This precursor was selected and used as recommended by **Toma, *et al.*** (2016) for non-conventional materials potentially suitable to obtain NPMs. After the 24-hour period, the medium had elapsed and we separated the lance and the iron solution obtained: one third in one beaker and the remaining two thirds in another one. Then, we slowly added 10 volumes of hydrogen peroxide to the beaker containing two-thirds of the iron solution until it changed from yellow to black. Subsequently, the black solution obtained was mixed with the remaining iron solution and a 5 M solution of NaOH in distilled water. The final mixture was stirred with a glass mixer to homogenize it until the black color was obtained again in the final product. The resulting NPMs were then separated using a neodymium magnet, decanted using acetone, and, finally, dried to remove the moisture. **Figure 3** shows an outline of this synthesis method.

We analyzed the morphology of the three totally dried nanoparticle samples by scanning electron microscopy in a Vega3 Tescan electronic microscope and we measured their size by implementing the free version of the ImageJ computational tool (**Schneider, *et al.*,** 2012).

The elemental characterization of the samples was performed using a Bruker XFlash® 410-M EDS probe coupled to the scanning electron microscope.

The structural characterization was carried out by X-ray diffraction (XRD) in a PANalytical X'Pert Pro diffractometer with a Co anode, a wavelength of Kα=1,789 Å, a current of 40 mA, and a voltage of 40 kV using the Bragg Brentano configuration with an angular step of 0.013° and an exposure time of 10 s.

## Results and discussion

### *Morphological characterization*

**Figure 4a**, obtained by scanning electron microscopy at 8.72 kX, shows the results for the synthesis method 1 revealing a random distribution of particles of different sizes with irregular granular formations of the particles and an average size of 2.31 ± 1.05 µm. Grey tones corresponding to the elements present in the sample Na, S, Cl, and Fe are evident in the image of backscattered electrons.


**Figure 3.** Simplified scheme of synthesis method 3

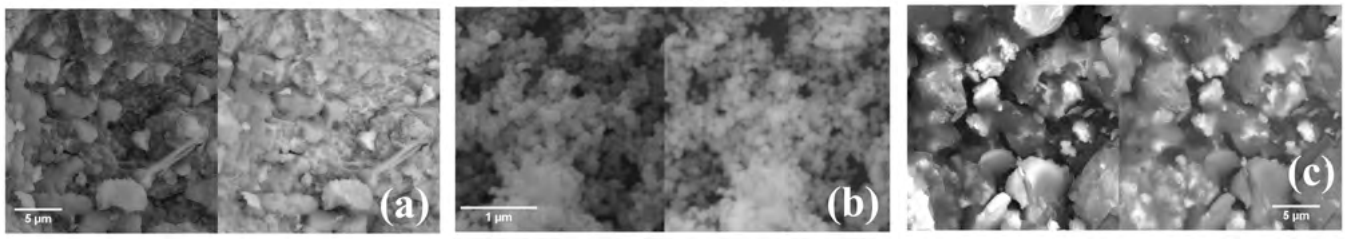


**Figure 4.** SEM micrographs of the samples. **(a)** Synthesis method 1, **(b)** Synthesis method 2, **(c)** Synthesis method 3

doi: https://doi.org/10.18257/raccefyn.1223

The results from the scanning electron microscopy at 70 kX for synthesis method 2 (**Figure 4b**) showed a spherical and uniform morphology. We calculated the average particle size obtaining a value of 104 ± 27 nm. These results are similar to those obtained by **Mohamad, *et al.*** (2020) where the glutathione catalyzed nano-magnetite particles appeared as scales and spheres with a particle size in the range of 50 to 100 nm. These results are also similar to those obtained by other researchers (**Shahid & Choi,** 2020; **Nurlilasari, *et al.*,** 2020).

Synthesis method 3 (**Figure 4c**) at 8.72 kX showed particles of irregular morphology with an average size of 4.03 ± 1.95 μm, which evidences that this method can produce micrometric particles due to the low speed of agitation used during the obtention process and the nature of the precursor elements.

***Composition***

In the spectrum of **figure 5a**, we observed a marked presence of Fe and O from which the possible formation of iron oxides can be inferred, as explained by **Rodríguez-López** (2012) in his doctoral work on the study of the synthesis and characterization of magnetite nanoparticles where he pointed out that this is the typical elemental composition of iron oxide particles. The appearance of elements such as Cl, S, and Na as residual traces of the precursors used in this method is evident as it has been reported in other studies by **Rodríguez-López, *et al.*** (2012) where they obtained magnetite particles using electrochemical methods.

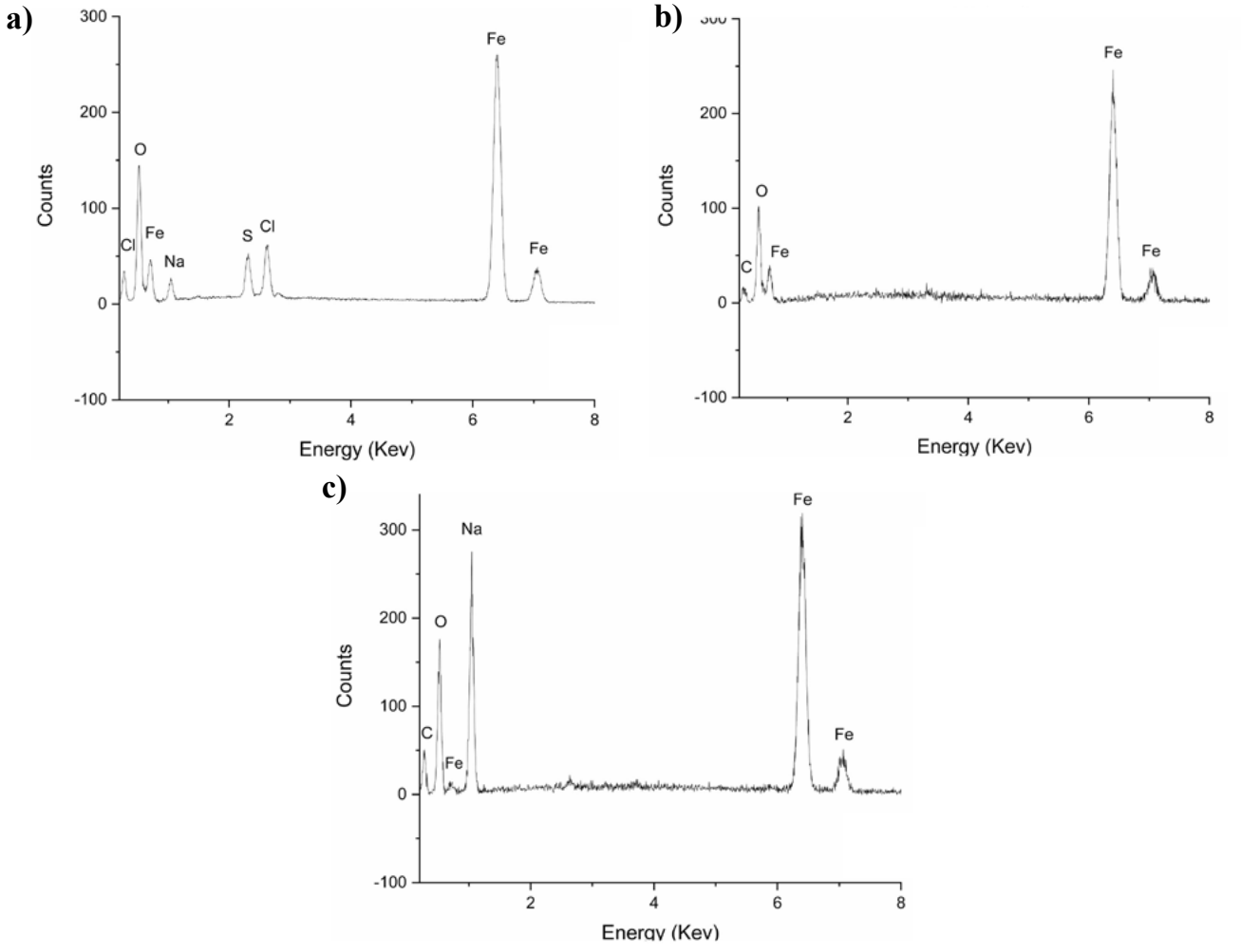


**Figure 5.** Elemental composition by EDS of the samples. **(a)** Synthesis method 1, **(b)** Synthesis method 2, **(c)** Synthesis method 3

doi: https://doi.org/10.18257/raccefyn.1223

The elemental composition shown in **figure 5b** corresponds to the sample obtained by using synthesis method 2, which presents a high purity since no peaks different from those of Fe and O are evident. However, the C, corresponding to the graphite tape used for the positioning of the powder in the scanning electron microscope camera, can be identified. Since the elements detected are Fe and O (as in method 1), we can infer that these particles correspond to iron oxides. This result is consistent with the investigations by **Yuan, *et al.*** (2020) where magnetite coatings were characterized.

The results of Method 3 are shown in **figure 5c** with the EDS spectrum showing a high presence of Fe, which indicates that these particles may be iron or iron oxides due, again, to the oxygen peak detected. The presence of Na, a product of the precursors, is strongly marked.

### *Structural characterization*

**Figure 6a** shows the diffractogram obtained for the sample synthesized by method 1 where the peaks corresponding to the crystalline structures of iron oxides are clearly observed. We also detected that the presence of magnetite was consistent with the diffraction pattern identified in the databases under ICDD No. 01-075-0449 and the magnetite identified under ICDD No. 00-025-1402. In **Shahid & Choi's** (2020b) study, the presence of these structures was evidenced in the samples obtained from industrial waste by inverse coprecipitation in the open air. Those samples showed magnetic behavior and structural results equivalent to those obtained in our study for the maghemite and magnetite phases.

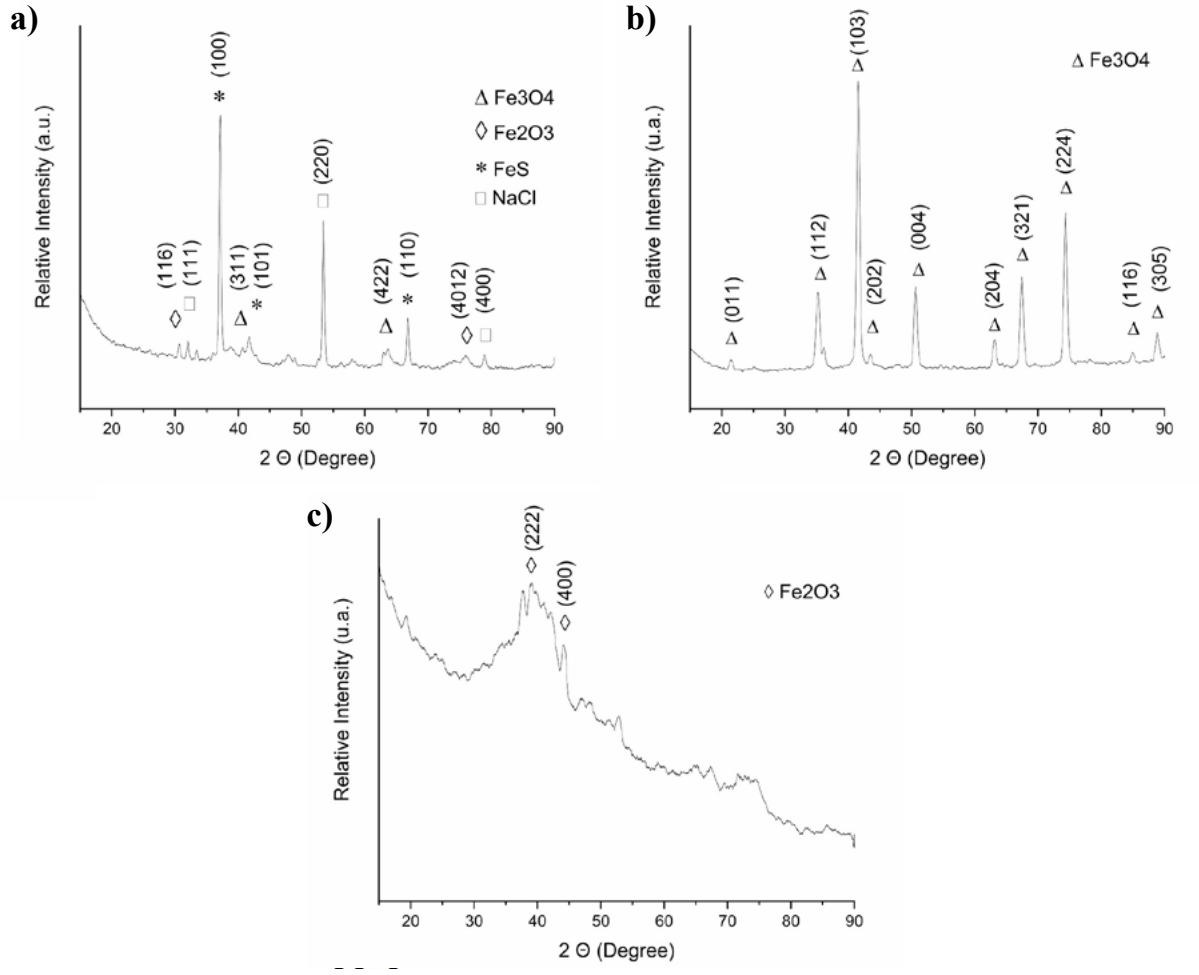


**Figure 6.** Diffractograms of the samples. **(a)** Synthesis method 1, **(b)** Synthesis method 2, **(c)** Synthesis method 3

doi: https://doi.org/10.18257/raccefyn.1223

As observed in the EDS, this sample had additional elements such as S, Cl, and Na, which formed crystalline salt structures such as NaCl matching the diffraction pattern identified by ICDD reference No. 00-002-0818 and FeS identified by ICDD reference No. 00-049-1632 in the process of obtention.

The diffractogram in **figure 6b** (synthesis method 2) allowed the identification of the formation of a single orthorhombic crystal structure present in the sample corresponding to the characteristic peaks of magnetite ($Fe_3O_4$). Those peaks matched with the diffraction pattern identified as ICDD reference No. 01-075-1609, an iron oxide known as magnetite with ferromagnetic behavior (**Noval, *et al.,*** 2017). This result is similar to the diffraction pattern obtained in the study conducted by **Singh, *et al.*** (2020) where they obtained and characterized magnetite-ZnO nanocomposites in which the magnetite had an equivalent diffraction pattern. In this sample, a greater definition of the diffraction peaks was observed due to the temperature used in the process, a similar behavior to that obtained by **Picasso, *et al.*** (2012) using low and high temperatures during the process for obtaining magnetite particles by sol-gel and coprecipitation.

The diffraction pattern in **figure 6c** corresponds to the sample obtained with synthesis method 3: A mostly amorphous structure and two peaks corresponding to the iron oxide known as maghemite (**Shokrollahi,** 2017) coinciding with the diffraction pattern identified with the ICDD reference No. 00-039-0238. **Patra, *et al.*** results (2019) were similar, as they obtained amorphous maghemite by direct solid-state synthesis. This type of structures, especially amorphous nanoparticles, have different physicochemical properties showing weaker magnetization responses than those shown by the same nanoparticles with a defined crystalline structure (**Hoang & Ganguli,** 2012).

Our results using methods 1 and 2 are consistent with those reported in the literature in terms of morphology and particle size, meaning they are easily accessed and developed to obtain maghemite and magnetite nanoparticles.

## Conclusions

The elemental composition of the samples analyzed by EDS primarily included Fe and O consistent with results reported in the literature regarding the composition of magnetic iron nanoparticles.

Method 2 did not present traces of any element other than Fe and O, however, methods 1 and 3 had traces of elements such as Na, S, and Cl, which are products of the precursors.

The samples obtained by method 2 showed crystalline magnetite structures while those obtained by synthesis method 1 showed structures of magnetite, maghemite, iron sulfide, and sodium chloride, and synthesis method 3 was characterized by the formation of an amorphous structure with small maghemite spikes.

These results showed that the obtention method has a great influence on the morphology and particle size with the sample obtained by method 2 being the most suitable in terms of its homogeneous, spherical, and nano-sized shapes up to 80 times smaller than those achieved by method 3 and up to 40 times smaller than those from method 1. These results open up a range of possibilities regarding the size, structure, and magnetic properties of the particles for future applications.

The physicochemical properties, particularly the magnetic ones, are affected by the presence of elements other than Fe and O, as well as the presence of an amorphous structure, a property that will be studied in future studies.

## Author contributions

NOG, DGAD, and JRR collaborated with the synthesis of the samples, compiled the EDS and SEM results, and wrote the manuscript; JRJ carried out the synthesis of the nanoparticles and carried out the structural characterization: DALT collaborated with the compositional and structural analysis of the samples.

## Conflicts of interest

The authors declare that there is no conflict of interest of any kind regarding the publication of the results of our research work.

## References

**Arévalo, P., Isasi, J., Caballero, A. C., Marco, J. F., Martín-Hernández, F.** (2017). Magnetic and structural studies of Fe3O4 nanoparticles synthesized via coprecipitation and dispersed in different surfactants. Ceramics International. **43** (13): 10333-10340. Doi: 10.1016/j.ceramint.2017.05.064

**Bakenecker, A. C., Ahlborg, M., Debbeler, C., Kaethner, C., Buzug, T. M., Lüdtke-Buzug, K.** (2020). Magnetic particle imaging in vascular medicine. Innovative Surgical Sciences. **3** (3): 179-192. Doi: 10.1515/iss-2018-2026

**Benhal, P., Broda, A., Najafali, D., Malik, P., Mohammed, A., Ramaswamy, B., Shapiro, B.** (2019). On-chip testing of the speed of magnetic nano- and micro-particles under a calibrated magnetic gradient. Journal of Magnetism and Magnetic Materials. **474** (November 2018): 187–198. Doi: 10.1016/j.jmmm.2018.10.148

**Blanco-Gutiérrez, V., Demourgues, A., Gaudon, M.** (2013). Sub-micrometric β-CoMoO4 rods: optical and piezochromic properties. Dalton Transactions. **42:** 13622-13627.

**Blanco-Gutiérrez, V., Saez-Puche, R., Torralvo-Fernández, M. J.** (2010). Magnetic behavior of ZnFe2O4 nanoparticles: Effects of a solid matrix and the particles size. Physical Chemistry C. **114:** 1789-1795.

**Chellappa, M., & Vijayalakshmi, U.** (2019). Fabrication of Fe 3 O 4 -silica core-shell magnetic nano-particles and its characterization for biomedical applications. Materials Today: Proceedings. **9:** 371-379. Doi: 10.1016/j.matpr.2019.02.166

**Hankiewicz, J. H., Stoll, J. A., Stroud, J., Davidson, J., Livesey, K. L., Tvrdy, K., … Celinski, Z. J.** (2019). Nano-sized ferrite particles for magnetic resonance imaging thermometry. Journal of Magnetism and Magnetic Materials. **469** (August 2018): 550-557. Doi: 10.1016/j.jmmm.2018.09.037

**Hoang, V. Van, & Ganguli, D.** (2012). Amorphous nanoparticles - Experiments and computer simulations. Physics Reports. **518** (3): 81-140. Doi: 10.1016/j.physrep.2012.07.004

**Houshiar, M., Zebhi, F., Razi, Z. J., Alidoust, A., Askari, Z.** (2014). Synthesis of cobalt ferrite (CoFe2O4) nanoparticles using combustion, coprecipitation, and precipitation methods: A comparison study of size, structural, and magnetic properties. Journal of Magnetism and Magnetic Materials. **371:** 43-48. Doi: 10.1016/j.jmmm.2014.06.059

**Iranmanesh, P., Tabatabai Yazdi, S., Mehran, M., Saeednia, S.** (2018). Superior magnetic properties of Ni ferrite nanoparticles synthesized by capping agent-free one-step coprecipitation route at different pH values. Journal of Magnetism and Magnetic Materials. **449:** 172-179. Doi: 10.1016/j.jmmm.2017.10.040

**Ismail M, A., Mostafa M, H., Sayed S, M.** (2019). Experimental and mathematical modeling of Cr(VI) removal using nano-magnetic Fe3O4-coated perlite from the liquid phase. Chinese Journal of Chemical Engineering. **(Vi):** 100632. Doi: 10.1016/j.neubiorev.2019.07.019

**Jin, L., Li, T., Wu, B., Yang, T., Zou, D., Liang, X., Zhang, J.** (2020). Rapid detection of Salmonella in milk by nuclear magnetic resonance based on membrane filtration super-paramagnetic nanobiosensor. Food Control. **110** (September 2019). Doi: 10.1016/j.foodcont.2019.107011

**Kisan, B., Shyni, P. C., Layek, S., Verma, H. C., Hesp, D., Dhanak, V., Perumal, A.** (2014). Finite size effects in magnetic and optical properties of antiferromagnetic NiO nanopartsicles. IEEE Transactions on Magnetics. **50** (1). Doi: 10.1109/TMAG.2013.2278539

**López-Ruiz, R., Magén, C., Luis, F., Bartolomé, J.** (2012). High temperature finite-size effects in the magnetic properties of Ni nanowires. Journal of Applied Physics. **112** (7). Doi: 10.1063/1.4756038

**Mohamad, N. D., Zaki, Z. M., Amir, A.** (2020). Mechanisms of enhanced oxidative degradation of tetrachloroethene by nano-magnetite catalysed with glutathione. Chemical Engineering Journal. **393** (March): 124760. Doi: 10.1016/j.cej.2020.124760

**Muñoz, F., Romero, A. H., Mejía-López, J., Morán-López, J. L.** (2013). Finite size effects on the magnetocrystalline anisotropy energy in Fe magnetic nanowires from first principles. Journal of Nanoparticle Research. **15** (4). Doi: 10.1007/s11051-013-1524-6

**Noval, V. E., Ochoa, C., Carriazo, J. G.** (2017). Magnetita, una estructura inorgánica con múltiples aplicaciones en catálisis heterogénea. Revista Colombiana de Quimica. **18:** 42-59. Doi: 10.15446/rev.colomb.quim.v1n1.62831

**Nurlilasari, P., Widiyastuti, W., Setyawan, H.** (2020). Novel monopolar arrangement of multiple iron electrodes for the large-scale production of magnetite nanoparticles for electrochemical reactors. Advanced Powder Technology. **31** (3): 1160-1168. Doi: 10.1016/j.apt.2019.12.043

**Patra, D., Gopalan, B., Ganesan, R.** (2019). Direct solid-state synthesis of maghemite as a magnetically recoverable adsorbent for the abatement of methylene blue. Journal of Environmental Chemical Engineering. **7** (5): 103384. Doi: 10.1016/j.jece.2019.103384

**Picasso, G., Vega, J., Uzuriaga, R., Ruiz, G. P.** (2012). Preparación de nanopartículas de magnetita por los métodos sol-gel y precipitación: estudio de la composición química y estructura. Revista de La Sociedad Química Del Perú. **78** (3): 170-182.

**Raeisi-Shahraki, R., Ebrahimi, M., Seyyed Ebrahimi, S. A., Masoudpanah, S. M.** (2012). Structural characterization and magnetic properties of superparamagnetic zinc ferrite nanoparticles synthesized by the coprecipitation method. Journal of Magnetism and Magnetic Materials. **324** (22): 3762-3765. Doi: 10.1016/j.jmmm.2012.06.020

**Ren, G., Yang, L., Zhang, Z., Zhong, B., Yang, X., Wang, X.** (2017). A new green synthesis of porous magnetite nanoparticles from waste ferrous sulfate by solid-phase reduction reaction. Journal of Alloys and Compounds. **710:** 875-879. Doi: 10.1016/j.jallcom.2017.03.337

**Rodríguez-López, A., Paredes-Arroyo, A., Mojica-Gomez, J., Estrada-Arteaga, C., Cruz-Rivera, J. J., Elías Alfaro, C. G., Antaño-López, R.** (2012). Electrochemical synthesis of magnetite and maghemite nanoparticles using dissymmetric potential pulses. Journal of Nanoparticle Research. **14** (8). Doi: 10.1007/s11051-012-0993-3

**Rodríguez-López, A.** (2012). Estudio de la síntesis y caracterización de nanopartículas de magnetita por métodos electroquímicos. Access date: September 15, 2012. Retrieved from: https://cideteq.repositorioinstitucional.mx/jspui/bitstream/1021/91/1/Estudiodelasíntesisy caracterización de nanopartículas de magnetita por métodos electroquímicos.pdf

**Schneider, C. A., Rasband, W. S., Eliceiri, K. W.** (2012). NIH Image to ImageJ: 25 years of image analysis. Nature Methods. **9** (7): 671–675. Doi: 10.1038/nmeth.2089

**Shahid, M. K. & Choi, Y.** (2020). Characterization and application of magnetite particles, synthesized by reverse coprecipitation method in open air from mill scale. Journal of Magnetism and Magnetic Materials. **495** (August 2019): 165823, p9. Doi: 10.1016/j.jmmm.2019.165823

**Shokrollahi, H.** (2017). A review of the magnetic properties, synthesis methods and applications of maghemite. Journal of Magnetism and Magnetic Materials. **426** (October 2016): 74-81. Doi: 10.1016/j.jmmm.2016.11.033

**Singh, H., Kumar, A., Thakur, A., Kumar, P., Nguyen, V. H., Vo, D. V. N., Kumar, D.** (2020). One-Pot Synthesis of Magnetite-ZnO Nanocomposite and Its Photocatalytic Activity. Topics in Catalysis. (0123456789). Doi: 10.1007/s11244-020-01278-z

**Sontu, U. B., G, N. R., Chou, F. C., M, V. R. R.** (2018). Temperature dependent and applied field strength dependent magnetic study of cobalt nickel ferrite nano particles: Synthesized by an environmentally benign method. Journal of Magnetism and Magnetic Materials. **452:** 398-406. Doi: 10.1016/j.jmmm.2018.01.003

**Tao, Y., Jiang, B., Yang, X., Ma, X., Chen, Z., Wang, X., Wang, Y.** (2020). Physicochemical study of the sustainable preparation of nano-Fe2O3 from ferrous sulfate with coke. Journal of Cleaner Production. **255**: 120175, p 9. Doi: 10.1016/j.jclepro.2020.120175

**Toma, H. E., Gomes da Silva, D., Condomitti, U.** (2016). *Nanotecnologia experimental*. São Paulo: Blucher. p. 63-85.

**Touqeer, T., Mumtaz, M. W., Mukhtar, H., Irfan, A., Akram, S., Shabbir, A., Yaw Choong, T. S.** (2020). Fe3O4-PDA-lipase as surface functionalized nano biocatalyst for the production of biodiesel using waste cooking oil as feedstock: Characterization and process optimization. Energies. **13** (1). Doi: 10.3390/en13010177

**Wang, L. & Zhang, M.** (2020). Study on synthesis and magnetic properties of Nd2Fe14B nanoparticles prepared by hydrothermal method. Journal of Magnetism and Magnetic Materials, 507(October 2019): 166841. Doi: 10.1016/j.jmmm.2020.166841

**Yuan, Z., Zhao, X., Meng, Q., Xu, Y., & Li, L.** (2020). Effect of selective coating of magnetite on improving magnetic separation of ilmenite from titanaugite. Minerals Engineering. 149 (May 2019): 106267, p 10. Doi: 10.1016/j.mineng.2020.106267